STRUCTURAL ANALYSIS OF SULFATE VEIN NETWORKS IN GALE CRATER (MARS)

Barbara De Toffoli [a,b,d*], Nicolas Mangold [b], Matteo Massironi [a,d], Alain Zanella [c]

Riccardo Pozzobon [a,d], Stephane Le Mouélic [b], Jonas L'Haridon [b], Gabriele Cremonese [d]

[a] Department of Geosciences, University of Padova, Via Gradenigo 6, Padova 35131, Italy

[b] Laboratoire de Planetologie et Geodynamique, Universite de Nantes, CNRS UMR 6112, Nantes, France

[c] Department of Geology, Université du Maine, Le Mans, France

[d] INAF, Osservatorio Astronomico di Padova, Vicolo dell'Osservatorio 3, Padova I-35122, Italy

* Corresponding author: tel. +39 3772678273, email: barbara.detoffoli@unipd.it & barbara.detoffoli@gmail.com

Abstract

The Curiosity rover's campaign in the Gale crater on Mars provides a large set of close-up images of sedimentary formations outcrops displaying a variety of diagenetic features such as light-toned veins, nodules and raised ridges. Through 2D and 3D analyses of Mastcam images we herein reconstruct the vein network of a sample area and estimated the stress field. Assessment of the spatial distribution of light-toned veins shows that the basin infillings, after burial and consolidation, experienced a sub-vertical compression and lateral extension coupled with fluid overpressure and cracking. Overall, rock failure and light-toned veins formations could have been generated by an overload produced by a pulse of infilling material within the basin.

Keywords: Mars – veins – fluid circulation – Curiosity rover – hydrofracturing

1. Introduction

NASA's Mars Science Laboratory mission, Curiosity, has been surveying the Gale crater since August 2012. It is equipped with a set of 17 cameras and 10 scientific instruments that allow rock and soil sample observation and analysis. Thanks to the *in situ* observations of the rover it has been possible to recognize fluid circulation features emplaced during diagenesis subsequent to burial and consolidation of the sediments. Specifically cross-cutting light-toned veins (Grotzinger et al., 2014, L'Haridon et al., 2018; Nachon et al., 2014, 2017), nodules (Stack et al., 2014) and raised ridges (Siebach et al., 2014; Léveillé et al., 2014; McLennan et al., 2014) were detected. According to ChemCam's Laser Induced Breakdown Spectroscopy (LIBS) measurements, the light-toned veins have a Ca-sulfate mineralogy (Nachon et al., 2014) mainly interpreted to be bassanite ($CaSO_4 \times 0.5\ H_2O$) at least on the surface exposed portions of the investigated outcrops (Rapin et al., 2016). These veins are observed throughout most of the outcrops recorded on the Curiosity traverse, especially in the fine-grained sandstones and mudstones, interpreted to be fluvial and lacustrine in origin (Grotzinger et al., 2014, 2015). The genesis of the veins is suggested to be ascribable to fluid flows that led to dissolution and re-precipitation of sulfate-rich materials (L'Haridon et al., 2018; Vaniman et al., 2018; Rapin et al., 2016; Schwenzer et al., 2016, Caswell and Milliken, 2017). Veins with mineral infilling are associated to two main stages of formation: i) the generation of fractures, which is a consequence of stresses and/or fluid overpressure produced by several factors such as fluid thermal expansion, the generation of fluid (i.e. diagenetic fluid expulsion), or chemical compaction; ii) the mineral infilling, which implies mineral dissolution, transport and precipitation that may occur to form single or multiple veins (e.g. Bjørlykke, 1997; Philipp, 2008; Zanella et al., 2020). Thus fluids, a material with suitable T and P conditions for dissolution at the original source to precipitation at the final outcropping location and fractures providing space for precipitation are the key ingredients to produce a network of mineral veins such as the ones observed at Gale crater.

The purpose of this study is to assess the structural behaviour recorded by a well-exposed crack system in a case study area along the rover traverse, to reconstruct the fracturing mechanisms, deduce the pattern of stress during fluid circulation and therefore provide some insights on the origin of the deformation involved during the formation of these features.

2. Geological Background

Gale is a complex crater located on the border of highlands close to the Martian dichotomy (5.37°S, 137.81°W) and filled by sedimentary deposits forming a central mound, Aeolis Mons (informally known as Mount Sharp). Gale crater is around 150 km in diameter and displays ~5 km of elevation difference between the floor and the central peak and rims (Young and Chan, 2017; Stack et al., 2016; Grotzinger et al., 2014, 2015; Le Deit et al., 2013; Wray, 2012). The meteor impact that formed Gale crater has been estimated to have occurred around the Noachian-Hesperian boundary (e.g. Le Deit et al., 2013; Thomson et al., 2011; Irwin et al., 2005). In the Late Noachian/Early Hesperian epoch a major climatic change led water to be increasingly unstable at surface conditions that Gale crater experienced and recorded (e.g. Le Deit et al., 2013). In fact, Gale crater has experienced an intricate evolution involving the past presence of surface water indicated by rim-crossing carved channels and lacustrine deposits at the mound base (e.g. Le Deit et al., 2013, Palucis et al., 2014, Grotzinger et al., 2014; Thomson et al., 2011; Milliken et al., 2010) and thus this site is considered invaluable for the paleoenvironment reconstruction and pivotal for the investigation of Martian habitability (e.g. Rubin et al., 2017, Caswell and Milliken, 2017).

Three main sedimentary groups have been identified in-situ by Curiosity rover investigations: the Bradbury group, the Mount Sharp group and the Siccar Point group (Fig.1; Grotzinger et al., 2014, 2015; Treiman et al., 2016). The first two groups are representative of a fluvio-lacustrine environment recorded by laminated and cross stratified mudstones, sandstones and pebble conglomerates, recognized especially at Pahrump Hills which is part of the Murray formation of

Mount Sharp group (e.g. Le Deit et al., 2016; Treiman et al., 2016; Stack et al., 2015; Bristow et al., 2015; Grotzinger et al., 2014, 2015). The third group is dominated by eolian sedimentary rocks that were accumulated unconformably over the other two and cemented (Banham et al., 2018).

Light-toned veins have been observed pervasively inside the Bradbury and Mount Sharp group at a varying frequency (Watkins et al., 2017, L'Haridon et al., 2018). Some veins cross the unconformity with the overlying eolian sedimentary rocks from the Siccar Point group (e.g. Frydenvang et al., 2017) showing that some of them formed well-after the cementation and erosion of the sedimentary layers. A remarkable part of the collected evidence related to the light-toned veins are based on the compositional information acquired with ChemCam (Maurice et al., 2012; Wiens et al., 2012) and its synergy with other instrument suites onboard Curiosity (e.g. CheMin, Chemical and Mineralogy, and MAHLI, Mars Hand Lens Imager). The light-toned veins have a calcium and sulfur-rich chemistry consistent with a Ca-sulfate mineralogy (Nachon et al., 2014), mainly interpreted to be bassanite from the analysis of the hydrogen emission line (Rapin et al., 2016).

The sedimentary rocks of interest for our work are located in the Murray formation, which is at the base of the Mount Sharp group. The Murray formation is composed of mudstones predominantly, with local fine-grained sandstones (Stein et al., 2018). An enhanced chemical alteration has been suggested from the presence of a large fraction of phyllosilicates (up to 25% in volume) and high values of chemical indices of alteration (Bristow et al., 2018, Mangold et al., 2019). The Murray mudstones have been affected by a widespread post-depositional history as observed through features such as fracture fills, veins, ridges and nodules, all indicating a complex diagenetic history, not limited to the light-toned veins focused in our study (Grotzinger et al., 2015, Nachon et al., 2017, L'Haridon et al., 2018). Investigating possible source of fluids that interplayed in fractures development would lead to a better understanding of the sulfate veins' origins (e.g. Schwenzer et al., 2016; Grotzinger et al., 2014, 2015, L'Haridon et al., 2018, Gasda et al., 2018). The source of sulfur for the sulfate veins filling the Murray mudstones is still unknown, but it has

been hypothesized to come from strata localized stratigraphically lower or higher than the mudstones, or from a lateral source (Grotzinger et al., 2014; McLennan et al., 2014; Nachon et al., 2015). Nevertheless, the facts that the fluid were mobilized by a late diagenetic event (Nachon et al., 2017; Young and Chan, 2017 and references therein) and that sulfate deposits have been identified from orbital data in layers above the Murray mudstones (Milliken et al., 2010), favour a source from younger sulfate-bearing sediments. Because of the ubiquitous presence of veins, a recent study proposed a paleoenvironmental evolution at the entire basin scale that could lead to deposition, accumulation, burial, dissolution and reprecipitation of the sulfates that filled the light-toned veins of Gale (Schwenzer et al., 2016). The light-toned veins of the Gale Crater seem to be similar to those observed in many sedimentary basins on Earth. This is especially the case for bedding-parallel fibrous gypsum veins called 'beef' veins (Buckland & De La Bèche, 1835) or 'BPV' for Bedding-parallel veins (e.g. Ukar et al., 2017). Several recent worldwide reviews demonstrate that these mineralized veins are very widespread on Earth, especially within impermeable and anisotropic materials such as mudstones (Cobbold et al., 2013; Gale et al., 2014; Zanella et al., 2020). These veins are interpreted to be the result of fluid-assisted fracturing due to pore fluid overpressures and stresses (e.g. Cobbold & Rodrigues, 2007; Cobbold et al., 2013). Indeed, the generation of distributed fluid overpressures explain the formation of horizontal tensile fractures that can be filled with minerals (e.g. Cobbold & Rodrigues, 2007; Mourgues et al. 2011; Zanella et al., 2014).

We collected structural data based on the distribution of light-toned veins distinguishable in the area that the Curiosity rover observed between sol (Martian days)1536 and 1545 (Fig.1a). While many outcrops of the Murray formation were either flat or partly buried below sand, this location was chosen because of the presence of clean blocks, less than 1 m high, where light-toned veins are visible enabling a detailed structural analysis using image analysis and photogrammetry helped by the large number of image available.

3. 3D reconstruction and measurements

To investigate the light-toned veins that have been detected in Gale crater we performed 2D and 3D analyses of Mastcam and Navcam Curiosity images. Mastcam takes colour images of 1600 × 1200 pixels that can be stitched together to create panoramas of the landscape around the rover. Mastcam consists of a two-camera system that can acquire true RGB colour images, using a Bayer filter, approximating what human eyes would perceive on Mars (Bell et al., 2012). With respect of the scientific purpose of Mastcam, the Navcam camera pairs were planned for operational use including acquisition of images for the rover's navigation, robotic planning and documentation, remote sensing science instrument pointing, but also general surface imaging (Maki et al., 2011). We coupled 2D mosaics of Mastcam images and the production of a 3D Digital Outcrop Model (DOM) (e.g. Caravaca et al., 2019) of the same region from both Mastcam and Navcam in order to reconstruct the fracture distribution in the area of interest which covers ~100 m^2 (Fig.2).

2D images were observed raw and stitched together, where overlapping acquisitions of neighbouring areas were available, in order to exploit full resolution image data for the detection of fractures' characterizing marks (e.g. junctions and lateral continuity) and local distributions in relation to other fracture sets and sediment laminations. We performed 3D reconstruction of the same investigated outcrops by means of the Agisoft software (Wagner et al., 2014) from multiple images taken by Mastcam binocular stereo vision and Navcam systems. Agisoft PhotoScan (recently renamed Metashape) is a 3D advanced modelling package based on image data processing which can automatically build the models without setting initial values and control points. It processes images taken at any position and angle as far adjacent photos share corresponding points recognizable on the targets. The scale computed by the software was tested by comparing it with known size objects such as rovers' wheels. Loading the images into Agisoft, the software automatically searches for the corresponding points matching and aligning the photos and finally generating a sparse point cloud. When the automatic alignment procedure failed, tie

points were manually implemented in the system to exploit the maximum number of images available. On the point cloud, that is generally denser closer to the observation point and favourably oriented surfaces, an irregular triangle net can be built, then the texture mapping is carried out according to the produced triangle net. We carried out the further step of elaboration by using the Cloud Compare environment, which is a 3D point cloud and triangular mesh processing software that allows the user to interact with 3D entities rotating, translating, drawing 2D polylines, picking points and extracting correspondent 2D and 3D information. In this context veins were marked by tracing polylines and further structural information (i.e. dip direction and dip angle, intersections angles, kinematics estimates) was developed by plane fitting and contextual data extraction through the Cloud Compare compass plugin.

Processing of structural data was carried out by means of Orient, a spherical projection and orientation data analysis software (https://www.frederickvollmer.com/orient/; Fig.3). Orient software allows to also perform kinematic and dynamic analysis of structural data including the generation of beachball plots (Fig.3e) and stress inversions (Fig.3c,d). The software is based on the Mohr–Coulomb failure criterion and automatically generates P and T axes, that indicate shortening and extension axes respectively. Fault plane lineation are not recognizable in our datasets, thus any extensional kinematic indicator detected along our veins (e.g. en-echelon tension gashes, micro pull-aparts, dilatational or constrictional step-overs) were assumed to be resolved on the related shear plane as a pure dip slip movement. Conjugate vein sets were interpreted according to the Andersonian theory of faulting which says that the maximum principal stress axis bisects the acute angle between them. Output data were finally plotted and beachball plots and paleostress distribution has been shown including confidence cones displayed by contours levels (in Figure 3 red contours highlight the 90% confidence intervals) (Erslev et al., 2004). We derived principal stress axes orientation from oblique vein sets (different groups of veins are discussed below in section 4).

4. Results

Both from 2D images and 3D reconstruction, the presence of different sets of non-randomly distributed fractures was neatly recognizable. All the fractures appear to have a higher resistance against erosion with respect of the host rock, in fact they tend to stick out from the knobs leading to an easy identification all over the outcrops. The first general distinction is the overall presence of one population of bedding-parallel light-toned veins and a second population of middle to high-angle dipping light-toned veins (Fig.4).

Bedding-parallel veins do not show significant thickness variations (averagely <1 cm) both at the single vein scale and among the general population, although lateral continuity is unclear and visible edges cropping out from the rocky knobs appear rounded and jagged. Bedding-parallel veins show a well recognizable average undulate, slightly wandering trend as recognizable in the measurements which display an averagely 12° ± 8 dipping angle variation range and a broad variability among the recorded dip directions (Fig3h) due to the variability of the available data, i.e. the outcropping visible veins, randomly sampling the undulate trend. Despite a consistently sub-horizontal and sub-parallel behaviour at the scale of the study area, bedding-parallel veins show in places a cross cutting relationship bending and stopping on the neighbouring ones (Fig.4b).

Oblique veins are less frequent than the sub-horizontal population (Fig.4). These veins display clear “en-echelon” structures well recognizable by the distinctive arrays of sigmoidal shaped cracks (Nicholson and Pollard, 1985), twisting out and bending as the result of mechanical interaction between tips of adjacent parallel cracks (Pollard et al. 1982). Such geometries are used to infer the state of deformation (Ramsay & Huber 1983) or the state of stress (Pollard et al. 1982, Rickard & Rixon 1983) in the surrounding rock at the time of cracking and accordingly, in the specificity of this case study, the “en-echelon” features are considered tensile veins opening in response to bulk non-coaxial shear whose extensional kinematics is displayed in figure 4a. We

measured two different sets of oblique cracks based on dip/dip-direction trends: (i) one with an average value of dip direction: 290°N and dip: 67° (spanning between minimum and maximum values of: 264°-309° dip direction and 54°-77° dip) and a (ii) second one showing a dip direction-dip average value of 155°N - 53° (spanning between minimum and maximum values of: 126°-184° dip direction and 31°-71° dip). On a vertical section (as the ones provided by the outcrops walls facing toward the Curiosity rover), the two populations of oblique fractures are thus intersecting at an average angle of 60° according to the measurements, as illustrated by single outcrops where fractures from both the oblique sets are visible (Fig.4).

In the study area it was also possible to observe cross-cutting relationships between the different sets above distinguished by orientation. No evidence of displacement was found and neither recurrent truncation of one set on the other were observed to determine an occurrence sequence (Fig.4d,e).

5. Discussions

On Mars, the combination of 2D and 3D products on the Gale crater floor with high-resolution in situ data along the rover track allows to pursue a structural interpretation of the basin at the time of the generation of the light-toned veins. The general trend of all the plane sets to crosscut the host rock laminations leads in first place to exclude a depositional layering interpretation. The presence of two cross-cutting sets of light-toned vein sets arranged ~60° apart and displaying en-echelon structures highlighting shear sense that led to a lowering of the hanging wall suggest an, at least partial, regime of extension. We exploited such vein sets to reconstruct the paleostress distribution by means of an automatic computational method implemented in the Orient software as discussed in section 3. Accordingly, the maximum principal stress is suggested to bisect the acute angle occurring between the sets that in the specificity of this case would mean that $\sigma 1$ lays

on a sub-vertical axis. The minimum σ3 orientation accordingly lays on a sub-horizontal plane and displays NW-SE direction (Fig.3).

The set of horizontal veins is well-matching disposition and morphology of failures induced by fluid overpressure recorded on Earth that happened during the fluid resurgence cracking the host rock along fresh planes or exploiting previously existing surfaces of weakness such as the mudstone bedding and laminations. In fact, as demonstrated theoretically by Cobbold & Rodrigues (2007) and experimentally by Mourgues et al. (2011), the generation of horizontal (bedding-parallel) fractures relates to fluid overpressure. In a sedimentary sequence, where no tectonic stress is applied, the principal stress σ1 is vertical due to the weight of the column of sediments itself while σ2 and σ3 are horizontal. In such situation, a distributed fluid overpressure will change the stress field, thus reducing or balancing σ1. As a consequence, the differential stress will be reduced and a local rotation of the stress field can occur and, if the fluid overpressure reaches the vertical lithostatic pressure and overcome the rock tensile strength, the generation of horizontal hydraulic tensile fractures can appear. Thus, fluid overpressure needs to have played a central role in the generation of the vein population herein discussed. Differently, we disfavour flows along local solubility gradients and/or chemical gradients and/or pressure solution and precipitation processes. In fact, the compositional information collected by the Curiosity MSL (Mars Science Laboratory) instrumentation do not favour the hypothesis of a chemical/solubility gradient interplay. ChemCam reported the presence of intermittent deposition of evaporitic or early diagenetic precipitation of sulfates in the Murray formation (Rapin et al., 2019). While these sulfates are faintly and locally detected, there are neither observed in the first 100 m of the Murray formation (where the studied outcrops are located) nor in the Bradbury formation while Ca-sulfate veins are also present. In addition, these depositional sulfates also contain Mg-sulfates thus it is to be expected, due to the high solubility of magnesium, that a solubility front from the host rock should also contain Mg-rich fluids, while veins have consistently shown only Ca-sulfates.

An example of the formation process that produced the horizontal vein set is the paleo-hydrofracturing model of gypsum veins in the lower Mercia Mudstone Group (Philipp, 2008). This group outcrops on the Somerset Coast of SW England, Watchet Bay, and display analogue characteristics to the rocks observed in the Gale crater (e.g. Young and Chan, 2017; Cobbold et al., 2013). The lower part of the Mercia Mudstone Group consists of several tens of meters of poorly bedded, red to reddish-brown unfossiliferous mudstones and siltstones (Whittaker and Green, 1983; Leslie et al., 1993), whereas in the upper part the red mudstones are characterized by laterally discontinuous evaporite-rich horizons, mainly composed of white nodular gypsum (Philipp, 2008). In the Mercia Mudstone Group vein dips show variations from horizontal to vertical and the strikes are in broad range of directions, no clear predominant attitude was detected. Crosscutting relationships were investigated as well and indicated no prevalent age relationship suggesting that the veins may all have formed at the same time (Philipp, 2008). The formation is interpreted to have formed in a playa lake or desert plain conditions (Bennison & Wright, 1969; Simms & Ruffell, 1990), where ephemeral pools were likely to be present and remobilization and accumulation of gypsum primarily disseminated in the sediment could have happened (Leslie et al., 1993). In Watchet Bay fluid transport took place mainly along faults and fractures since mudstones have a very low original permeability and are commonly effective barriers to fluid circulation (Philipp, 2008; Cartwright, 1997). The outcrops show discontinuous anastomosing networks of gypsum veins confined to portions of the hosting mudstone. The phenomenon is not pervasive to the whole mudstone group though, but it is confined to specific portions often overlain by thick grey siltstone layers weakly calcareous (Philipp, 2008). It may in fact occur that veins produced by hydrofracturing stop where mechanical contrast boundaries occur (e.g. Brenner and Gudmundsson, 2004b; Gudmundsson et al., 2002; Cosgrove, 2001; Gudmundsson and Brenner, 2001). There is no need of active slipping faults to allow fluid circulation and hydrofracturing, that are triggered when the pressure of the fluids sited within the veins exceed the lithostatic pressure (Ramsey, 1980). When fluids are involved (e.g. geothermal fluids), buoyancy overpressure can

convey a significant contribution to the fracturing process. Depending on the stress field, fluids can be transported along the veins (i) leading to hydrofracturing propagation of already existing fracture planes and anisotropies (i.e. bedding planes and laminations) or (ii) generating hydrofracturing into the host rock (Philipp, 2008 and references therein). Philipp (2008) suggests an hydrofracturing model to explain the sulphate vein network systems that cut the Mercia Mudstone Group based on low permeability of the mudstone that drove fluids, flowing from the highest to the lowest hydraulic potential (Domenico & Schwartz, 1998), to enter the rocks along faults and fractures and prevented them to penetrate intimately the host rock.

Even if the Martian dynamics are less constrained with the respect of their terrestrial counterparts, we interpret a diffuse fluid overpressure as the primary cause of vein formation due to peculiar recognised vein traits such as: (i) the absence of abrupt terminations or thickness variations of sub-horizontal veins in correspondence with undulation of the bedding planes (potentially indicating local pressure-solution and precipitation processes); (ii) the absence of structures due to inter bedding shear and/or flexural slip which could have had eventually facilitated local dissolution or precipitation processes; (iii) recorded cross cutting relationship with the host rock laminations; (iv) the large abundance of bedding-parallel veins with the respect of the oblique ones; and (v) veins' Ca sulphate composition differing from the primary Ca-Mg sulphates of the Murray formation indicating an external source of the precipitated material. Moreover, a certain overburden is likely to have been in place at the moment of the vein formation. The study area depth at the moment of the vein formation is not known, but it could have reached a maximum depth of 3 to 5 kilometres based on crater rim minimum and maximum elevation (Le Deit et al., 2013). Accordingly, the maximum overburden load (referred to an average sandstone density of 2 323 kg/m^3) during vein formation could have reached a range between 0.25 to 0.43 MPa. In such scenario, to crack the host rock during hydrofracture propagation, the tensile strength of the material needs be taken into account. According to the work of Philipp (2012) the sum of the lithospheric pressure (p_l) and the fluid overpressure at the location where hydrofracturing takes

place (p_e) equals the sum of the stress opposing the opening (σ_x) and the tensile strength of the rock (T). Eq (1):

$$p_l + p_e = \sigma_x + T \qquad (1)$$

In the case study herein discussed, horizontal veins needed to overcome σ1 to open which is represented by the lithostatic pressure. Accordingly, the minimum fluid overpressure needed to open the veins equals the tensile strength of the cracked material, i.e. mudstones that display average tensile strength values around 5.4 MPa (Perras and Diederichs, 2014).

The fluid source for the Martian case study is not entirely clear; fluid flow can be triggered by very diverse physical and chemical disequilibria that might generate fluid overpressure. Some examples could be compaction due to burial, diagenetic fluid expulsion and buoyancy, crystallization, porosity changes and thermal expansion (Neuzil, 1995; Bjørlykke, 1997; Osborne & Swarbrick, 1997). On Mars, Gale experienced water-rich early stages (Late Noachian/Early Hesperian) during which the crater could have been connected to both surficial and underground water reservoirs (e.g., Villanueva et al. 2015; Andrews-Hanna et al., 2010), thus implying potentially transient flooding and drying in sabkha or ephemeral lake environments leading to mineral (e.g. salts) precipitation and accumulation in the basin (Rapin et al., 2019).

Nevertheless, these veins are not likely to have formed early in the basin history, but when compaction, consolidation and diagenetic processes started affecting the region. In fact a significant part of the vein population consists of well recognisable fractures cross-cutting rock bedding (both from oblique and bedding-parallel vein sets, this is particularly well visible in the sub-horizontal vein sample highlighted in figure 4c), hence the mudstone must have had some tensile strength at the time of formation to trigger a brittle response thus excluding a young soft host rocks (Schwenzer et al., 2016; Philipp, 2008; Bell, 2000). Thus, subsequent dissolution and mobilization by diagenetic fluids of initial deposits, of unclear stratigraphic position yet, may have led to the formation of the sulphate veins observed on the rover traverse (L'Haridon et al., 2018; Schwenzer et al., 2016; Nachon et al., 2017; Grotzinger et al., 2014; McLennan et al., 2014).

Additionally, the observed veins are late stage because, at least some of them, crosscut the unconformity into the overlying Stimson unit that is an eolian unit formed much later (Rapin et al., 2019).

6. Conclusions

Light-toned fracture networks have been observed repeatedly along Curiosity rover traverse (e.g. Watkins et al., 2017) and their distribution reflects the stress field they have been exposed to at the moment of fracturing. Within the window of ten sols (sol 1536 – sol 1545) herein analysed, Curiosity acquired a large number of images from different angles of a field of bedrock knobs cropping out from the sand where many sulphate veins were neatly visible. This asset allowed the 3D reconstruction of the area and, contextually, the 3D reconstruction of the plane set where fractures lay. On Earth, similar arrangements can be observed at Watchet Bay where networks of intersecting sulphate veins developed thanks to hydrofracturing regimes within reddish mudstone levels.

In Gale, the fracturing process is therefore to be ascribed to two different complementary contributions: (i) the 60° dipping fractures are to be considered the product of a combination of both fluid overpressures and an extensional regime where the principal stress lays on a vertical axis and a shear component was present (Fig.4a); (ii) the set of bedding-parallel fractures are the result of a hydrofracturing process where the distributed fluid overpressure was energetic enough to open and fill fractures, largely (but not exclusively) following pre-existing weakness surfaces constituted by mudstone layering. Additionally, the formation of the bedding-parallel vein set might have been synchronous to the formation of the other two sets since no truncation or displacement have been observed around the available outcrops. This interpretation is well supported by the geological context. Gale is a large crater that experienced water and sediment infilling, the vertical maximum stress is reasonably to be ascribed to such progressive overload.

The cracking drive of hydrofracturing, can be triggered either by the emplacement of an overburden that perturbs fluid pressure, or as response to an unloading event when pressurized fluids are already stored in the subsurface. The origin of fluids at Gale is still debated and overpressure cracking itself does not carry enough information to discriminate it. In the hypothesis of a coeval genesis of the oblique and the bedding-parallel vein networks, a pulse of material overload or progressive compaction within the crater could have been responsible both for the extensional failure and the fluid escape from the already consolidated deposits on the crater floor. In fact, Gale crater experienced episodes of lacustrine environment during its late stages of activity, far after the deposition of the mudstones in which fractures are observed (as pointed out by the presence of fan deposits, Palucis et al., 2016). Hence continuous deposition and eventual multiple material pulses are likely to have took place during the crater history and had the potential to contribute to the vein generation. In this context, due to the crater circular shape, maximum extension is accordingly expected to develop along the radial directions. This is confirmed by σ3 NE-SW direction recorded in the study area, σ3 thus locally appears to develop radially compared to the closest crater rim. However, to better constrain the scenario, it would be necessary to collect data from multiple sites along the rover traverse in order to check the behaviour of σ3 at different position with the respect of the crater rim.

Veins mapping and reconstruction allowed the production of a well constrained structural context interpretation and cracking driving forces identification which are likely to have been active in the whole crater area so producing a structural context for the entirety of the fracture and vein networks that have been recorded along the rover traverse.

Acknowledgments

This paper is part of a project supported by the European Union's Horizon 2020 research and innovation program under grant agreement Nº776276 (PLANMAP) and has been supported by the "Fondazione Ing. Aldo Gini" scholarship. Some of the authors were funded by the Centre National

d'Etudes Spatiales (CNES). The data reported in this paper are archived at the Planetary Data System, accessible at http://pds-geosciences.wustl.edu/missions/msl/index.htm. We are indebted to the Mars Science Laboratory Project engineering and science teams for their diligent efforts in making the mission as effective as possible and for their participations in tactical and strategic operations.

References

Andrews-Hanna, J.C., et al., 2010. Early Mars hydrology: Meridiani playa deposits and the sedimentary record of Arabia Terra. J. Geophys. Res. E Planets 115, 1–22. https://doi.org/10.1029/2009JE003485

Banham, S. G. et al. (2018) Ancient Martian aeolian processes and palaeomorphology reconstructed from the Stimson formaton on the lower slope of aeolis Mons, Gale Crater, Mars, Sedimentology, 65, 993-1042.

Bell, F. G., 2000. Engineering Properties of Soils and Rocks. Oxford: Blackwell.

Bell, J. F., et al., 2012. Mastcam multispectral imaging on the Mars Science Laboratory rover: wavelength coverage and imaging strategies at the gale crater field site, Lunar Plan. Sci. Conference, pp 2541

Bennison, G. M. and Wright, A. E. 1969. The Geological History of the British Isles. London: Edward Arnold Ltd, 406 pp.

Bjørlykke, K. 1997. Lithological control on fluid flow in sedimentary basins. In Fluid Flow and Transport in Rocks (eds B. Jamtveit & B. W. D. Yardley), pp. 15– 34. London: Chapman and Hall.

Brenner, S. L. & Gudmundsson, A. 2004b. Arrest and aperture variation of hydrofractures in layered reservoirs. In The Initiation, Propagation and Arrest of Joints and Other Fractures (eds J. W. Cosgrove & T. Engelder), pp. 117–28. Geological Society of London, Special Publication no. 231.

Bristow, T. F., et al., 2015. The origin and implications of clay minerals from Yellowknife Bay, Gale crater, Mars, Am. Mineral., 100, 824–836, doi:10.2138/am-2015-5077CCBYNCND.

Buckland and De la Beche, 1835. On the Geology of the Neighbourhood of Weymouth and the Adjacent Parts of the Coast of Dorset Transactions of the Geological Society, London 2–4, pp. 1–46

Caravaca, G.; Le Mouélic, S.; Mangold, N.; L'Haridon, J.; Le Deit, L.; Massé, M., 2019. 3D Digital Reconstruction of the Kimberley Outcrop (Gale Crater, Mars) from Photogrammetry Using Multi-Scale Imagery from Mars Science Laboratory 50th Lunar and Planetary Science Conference

Cartwright, J. A. 1997. Polygonal extensional fault systems: a new class of structure formed during the early compaction of shales. In Fluid Flow and Transport in Rocks (eds B. Jamtveit & B. W. D. Yardley), pp. 35–56. London: Chapman & Hall.

Caswell, T.E., Milliken, R.E., 2017. Evidence for hydraulic fracturing at Gale crater, Mars: implications for burial depth of the Yellowknife Bay formation. Earth Planet. Sci. Lett. 468, 72–84. doi:10.1016/j.epsl.2017.03.033.

Cobbold, P.R., Zanella, A., Rodrigues, N., Løseth, H., 2013. Bedding-parallel fibrous veins (beef and cone-in-cone): worldwide occurrence and possible significance in terms of fluid overpressure, hydrocarbon generation and mineralization, Mar. Pet. Geol., 43, pp. 1-20, 10.1016/j.marpetgeo.2013.01.010

Cobbold, P.R., Rodrigues, N., 2007. Seepage forces, important factors in the formation of horizontal hydraulic fractures and bedding-parallel fibrous veins ("beef" and "cone-in-cone"), Geofluids, 7, pp. 313-322, 10.1111/j.1468-8123.2007.00183.x

Cosgrove, J.W., 2001. Hydraulic fracturing during the formation and deformation of a basin: A factor in the dewatering of low-permeability sediments. Am. Assoc. Pet. Geol. Bull. 85, 737–748. https://doi.org/10.1306/8626C997-173B-11D7-8645000102C1865D

Domenico, P. A. & Schwartz, F. W. 1998. Physical and Chemical Hydrogeology, 2nd ed. New York: Wiley, 506

Erslev, E.A., Holdaway, S.M., O'Meara, S.A., Jurista, B., and Selvig, B., 2004. Laramide minor faulting in the Colorado Front Range. New Mexico Bureau of Geology & Mineral Resources Bulletin, v. 160, p. 181-203.

Frydenvang J. et al., 2017. Diagenetic silica enrichment and late-stage groundwater activity in Gale crater, Mars. Geophys. Res. Let., 44, 4716-4724.

Gale, J.F.W., Laubach, S.E., Olson, J.E., Eichhubl, P., FallA., 2014. Natural fractures in shale: A review and new observations, AAPG Bulletin, 98 (11): 2165–2216. doi: https://doi.org/10.1306/08121413151

Gasda, P. J., et al. (2017) In situ detection of boron by ChemCam on Mars, Geophysical Research Letters, 44, 8739-8748.

Grotzinger, J.P., et al., 2014. A habitable fluvio-lacustrine environment at Yellowknife Bay, Gale crater, Mars. Science (80–) 343 (6169). 1242777–1242777 doi: 10.1126/ science.1242777.

Grotzinger, J.P., et al., 2015. Deposition, exhumation, and paleoclimate of an ancient lake deposit, Gale crater, Mars. Science (80–) 350 (6257). aac7575-aac7575 doi: 10.1126/science.aac7575.

Gudmundsson, A. & Brenner, S. L. 2001. How hydrofractures become arrested. Terra Nova 13, 456–62.

Gudmundsson, A., et al., 2002. Propagation pathways and fluid transport of hydrofractures in jointed and layered rocks in geothermal fields. Journal of Volcanology and Geothermal Research 116, 257–78.

Hurowitz, J.A., Grotzinger, J.P., Fischer, W.W., McLennan, S.M., Milliken, R.E., Stein, N., Vasavada, A.R., Blake, D.F., Dehouck, E., Eigenbrode, J.L., Fairén, A.G., Frydenvang, J., Gellert, R., Grant, J.A., Gupta, S., Herkenhoff, K.E., Ming, D.W., Rampe, E.B., Schmidt, M.E., Siebach, K.L., Stack-Morgan, K., Sumner, D.Y., Wiens, R.C., 2017. Redox stratification of an ancient lake in Gale crater, Mars. Science (80-.). 356. https://doi.org/10.1126/science.aah6849

Irwin, R. P., A. D. Howard, R. A. Craddock, and J. M. Moore (2005), An in- tense terminal epoch of widespread fluvial activity on early Mars: 2. Increased runoff and paleolake development, J. Geophys. Res., 110, E12S15, doi:10.1029/2005JE002460.

L'Haridon, J., Mangold, N., Meslin, P.-Y., Johnson, J. R., Rapin, W., Forni, O., et al. (2018). Chemical variability in mineralized veins observed by ChemCam on the lower slopes of Mount Sharp in Gale crater, Mars. Icarus, 311, 69–86. https://doi.org/10.1016/j.icarus.2018.01.028

Le Deit, L., E. Hauber, F. Fueten, M. Pondrelli, A. P. Rossi, and R. Jaumann (2013), Sequence of infilling events in Gale Crater, Mars: Results from morphology, stratigraphy, and mineralogy, J. Geophys. Res. Planets, 118, doi:10.1002/ 2012JE004322.

Le Deit, L., et al., 2016. The potassic sedimentary rocks in Gale crater, Mars, as seen by ChemCam on board Curiosity. J. Geophys. Res. Planets 121 (5), 784–804. doi:10.1002/2015JE004987.

Leslie, A. B., et al., 1993. Geochemical and mineralogical variations in the upper Mercia Mudstone Group (Late Triassic), southwest Britain: correlation of outcrop sequences with borehole geophysical logs. Journal of the Geological Society, London 150, 67–75.

Léveillé, R.J., et al., 2014. Chemistry of fracture-filling raised ridges in Yellowknife Bay, Gale crater: window into past aqueous activity and habitability on Mars. J. Geophys. Res. Planets 119 (11), 2398–2415. doi:10.1002/2014JE004620.

Maki, J. N., et al., 2011. The Mars Science Laboratory (Msl) Navigation Cameras (Navcams), Lunar Plan. Sci. Conference, pp 2738

Mangold, N., Dehouck, E., Fedo, C., Forni, O., Achilles, C., Bristow, T., Downs, R.T., Frydenvang, J., Gasnault, O., L'Haridon, J., Le Deit, L., Maurice, S., McLennan, S.M., Meslin, P.Y., Morrison, S., Newsom, H.E., Rampe, E., Rapin, W., Rivera-Hernandez, F., Salvatore, M., 2019. Chemical alteration of fine-grained sedimentary rocks at Gale crater. Icarus 321, 619–631.

Marrett, R., and Allmendinger, R.W., 1990. Kinematic analysis of fault-slip data. Journal of Structural Geology, v. 12, p. 973-986.

Maurice, S. and 69 co-authors, 2012. The ChemCam instrument suite on the Mars Science Laboratory (MSL)

rover: Science objectives and mast unit description. Space Sci. Rev., 170 :95-166, doi 10.1007/s11214-012-9912-2.

McLennan, S.M., et al., 2014. Elemental geochemistry of sedimentary rocks at Yel- lowknife Bay, Gale crater, Mars. Science (80–) 343 (6169), 1244734. doi:10.1126/ science.1244734.

Milliken, R.E., et al., 2010. Paleoclimate of Mars as captured by the stratigraphic record in Gale crater. Geophys. Res. Lett. 37 (4), 1–6. doi:10.1029/2009GL041870.

Mourgues, R., Gressier, J. B., Bodet, L., Bureau, D., & Gay, A., 2011. "Basin scale" versus "localized" pore pressure/stress coupling–Implications for trap integrity evaluation. Marine and Petroleum Geology, 28(5), 1111-1121.

Nachon, M., et al., 2014. Calcium sulfate veins characterized by ChemCam/Curiosity at Gale crater, Mars. J. Geophys. Res. Planets 119 (9), 1991–2016. doi:10.1002/ 2013JE004588.

Nachon, M., et al., 2017. Chemistry of diagenetic features analyzed by ChemCam at Pahrump Hills, Gale crater, Mars. Icarus 281, 121–136. doi:10.1016/j.icarus.2016.08. 026.

Neuzil, C. E. 1995. Abnormal pressures as hydrodynamic phenomena. American Journal of Science 295, 742–86.

Nicholson, R. & Pollard, D.D. 1985. Dilation and linkage of en-echeleon cracks. Journal of Structural Geology, 7, 583–590.

Osborne, M. J. & Swarbrick, R. E. 1997. Mechanisms for generating overpressure in sedimentary basins: A reevaluation. American Association of Petroleum Geologists Bulletin 81, 1023–41.

Palucis, M., W. Dietrich, A. Hayes, R. Williams, S. Gupta, N. Mangold, H. E. Newsom, C. Hardgrove, F. Calef, D. Sumner, 2014, The origin and evolution of the Peace Vallis fan system that drains to the Curiosity landing area, Gale Crater, Mars, J. Geophys. Res. Planets, 119, 705–728, doi:10.1002/2013JE004583

Palucis, M., W. E. Dietrich, R. M. E. Williams, A. G. Hayes, T. Parker, D. Y. Sumner, N. Mangold, K. Lewis, and H. Newsom, 2016. Sequence andrelative timing of large lakes in Gale crater (Mars) after the formation of Mt. Sharp, J. Geophys. Res. Planets, 121, 472 –496, doi:10.1002/2015JE004905.

Perras, M.A., Diederichs, M.S., 2014. A Review of the Tensile Strength of Rock: Concepts and Testing. Geotech. Geol. Eng. 32, 525–546. https://doi.org/10.1007/s10706-014-9732-0

Phillip, S. L., 2008. Geometry and formation of gypsum veins in mudstones at Watchet, Somerset, SW England, Geol. Mag., 145(6), 831–844, doi:10.1017/S0016756808005451.

Philipp, S.L., 2012. Fluid overpressure estimates from the aspect ratios of mineral veins. Tectonophysics 581, 35–47. https://doi.org/10.1016/j.tecto.2012.01.015

Pollard, D. D., Segall, P. & Delaney, P. T. 1982. Formation and interpretation of dilatant echelon cracks. Bull.

geol, Soc. Am. 93, 1291-1303.

Rapin, W., et al., 2016. Hydration state of calcium sulfates in Gale crater, Mars: iden- tification of bassanite veins. Earth Planet. Sci. Lett. 452, 197–205. doi:10.1016/j. epsl.2016.07.045.

Rapin, W., Ehlmann, B.L., Dromart, G. et al. 2019. An interval of high salinity in ancient Gale crater lake on Mars. Nat. Geosci. 12, 889–895. https://doi.org/10.1038/s41561-019-0458-8

Ramsay, J. G. 1980. The crack-seal mechanism of rock deformation. Nature 284, 135–9

Ramsay, J. G. & Huber. M. I. 1983. The Techniques of Modern Structural Geology, Volume 1, Basic Techniques--Strain Analysis. Academic Press, London.

Rickard, M. J. & Rixon, L. K. 1983. Stress configurations in conjugate quartz-vein arrays. J. Struct. Geol. 5,573-578.

Rubin, D.M., et al., 2017. Fluidized-sediment pipes in Gale crater, Mars, and possible Earth analogs. Geology 45, 7–10. https://doi.org/10.1130/G38339.1

Schwenzer, S.P., et al., 2016. Fluids during diagenesis and sulfate vein formation in sediments at Gale crater, Mars. Meteorit. Planet. Sci. 28. doi:10.1111/maps. 12668.

Siebach, K.L., Grotzinger, J.P., Kah, L.C., Stack, K.M., Malin, M., Léveillé, R., Sum- ner, D.Y., 2014. Subaqueous shrinkage cracks in the Sheepbed mudstone: im- plications for early fluid diagenesis, Gale crater, Mars. J. Geophys. Res. Planets 119 (7), 1597–1613. doi:10.1002/2014JE004623.

Simms, M. J. and Rufell, A. H. 1990. Climatic and biotic change in the late Triassic. Journal of the Geological Society, London 147, 321–7

Stack, K.M., et al., 2014. Diagenetic origin of nodules in the Sheepbed member, Yellowknife Bay formation, Gale crater, Mars. J. Geophys. Res. Planets 119 (7), 1637– 1664. doi:10.1002/2014JE004617.

Stack, K. M., et al., 2015. Sedimentology and stratigraphy of the Pahrump Hills outcrop, lower Mount Sharp, Gale Crater, Mars, 46 calcium sulfate veins as observed by the ChemCam instrument, 46 Planetary Science Conference, 2 pp.

Stack, K. M., et al. 2016. Comparing orbiter and rover image-based mapping of an ancient sedimentary environment, Aeolis Palus, Gale crater, Mars, Icarus, doi:10.1016/j.icarus.2016.02.024.

Thomson, B.J., et al., 2011. Constraints on the origin and evolution of the layered mound in Gale crater, Mars using Mars Reconnaissance Orbiter data. Icarus 214 (2), 413–432. doi:10.1016/j.icarus.2011.05.002

Treiman, A.H., et al., 2016. Mineralogy, provenance, and diagenesis of a potassic basaltic sandstone on Mars: CheMin X-ray diffraction of the Windjana sam- ple (Kimberley area, Gale crater). J. Geophys. Res. Planets 121 (1), 75–106. doi:10.1002/2015JE004932.

Ukar, E., Lopez, R.G., Laubach, S.E., Gale, J.F.W., Manceda, R., Marrett R., 2017. Microfractures in bed-parallel veins (beef) as predictors of vertical macrofractures in shale: Vaca Muerta Formation, Agrio Fold-and-Thrust Belt, Argentina, Journal of South American Earth Sciences, 79, pp. 152-169, 10.1016/j.jsames.2017.07.015

Vaniman, D.T., et al., 2018. Gypsum, bassanite, and anhydrite at Gale crater, Mars. Am. Mineral. 103, 1011–1020. https://doi.org/10.2138/am-2018-6346

Villanueva G. L. et al., 2015. Strong water isotopic anomalies in the Martian atmosphere: Probing current and ancient reservoirs. Science 348:218–221.

Wagner, R. V., Henriksen, M.R., Manheim, M.R., Robinson, M.S., 2014. Photoscan for Planetary and Analogues Sites, in: 3rd Planetary Data Workshop. p. 7023. https://doi.org/10.1016/j.icarus.2014.04.002

Watkins, J. A., et al., 2017. Fracture formation by compaction-related burial in Gale crater, Mars: implications for the origin of Aeolis Mons, Lunar Plan. Sci. Conference, pp 3019

Whittaker, A. and Green, G. W. 1983. Geology of the country around Weston-super-Mare, memoir for 1:50,000 geological sheet 279. New series, with parts of sheet 263 and 295. Geological Survey of Great Britain, Institute of Geological Sciences. London: Her Majesty's Stationery Office, 147 pp.

Wiens, R. C. and 80 co-authors, 2012. The ChemCam instrument suite on the Mars Science Laboratory (MSL) rover: body unit and combined systems, Space Sci. Rev., 170 :167-227, doi 10.1007/s11214-012-9902-4.

Wray, J. J., 2012. Gale crater: The Mars Science Laboratory/Curiosity Rover Landing Site, Int. J. Astrobiol., doi:10.1017/S1473550412000328.

Young, B.W., Chan, M.A., 2017. Gypsum veins in Triassic Moenkopi mudrocks of southern Utah: Analogs to calcium sulfate veins on Mars. J. Geophys. Res. 150–171. https://doi.org/10.1002/2016JE005118

Zanella, A., Cobbold, P.R., & Le Carlier de Veslud, C., 2014. Physical modelling of chemical compaction, overpressure development, hydraulic fracturing and thrust detachments in organic-rich source rock. Marine and Petroleum Geology, 55, 262-274. doi:10.1016/j.marpetgeo.2013.12.017.

Zanella, A., Cobbold, P.R., Rodrigues, N., Loseth, H., Jolivet, M., Gouttefangeas, F., Chew, D..Source rocks in foreland basins: a preferential context for the development of natural hydraulic fractures. AAPG Bulletin, in press.

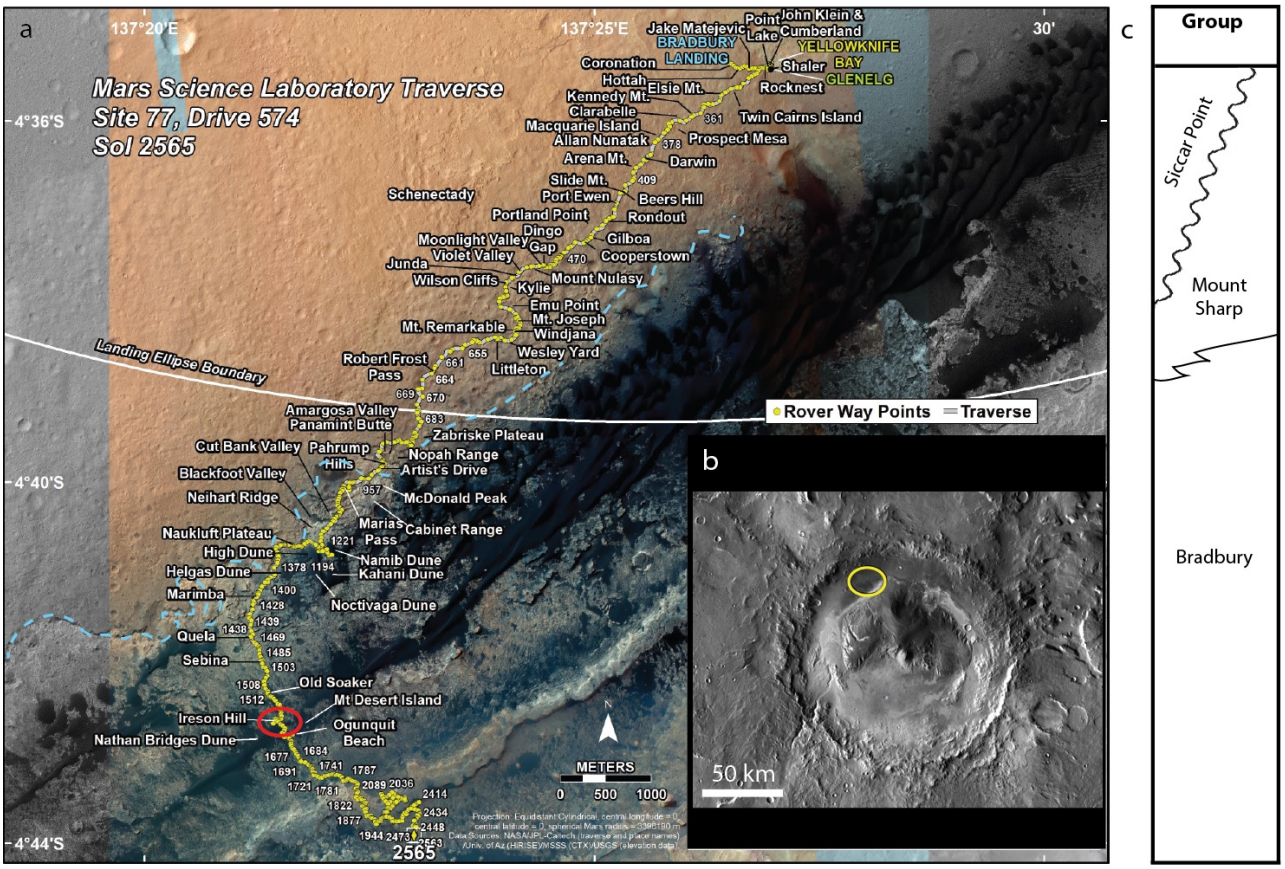

Figure 1. In panel (a) the yellow line with stops displays the Curiosity rover traverse; in the red circle the study area is highlighted; the blue dashed line represents the contact between the Bradbury group (NW) and the Mount Sharp group (SE). (b) Gale crater surveyed region. (c) Stratigraphic column of Gale crater sedimentary rocks (modified after Hurowitz et al., 2017).

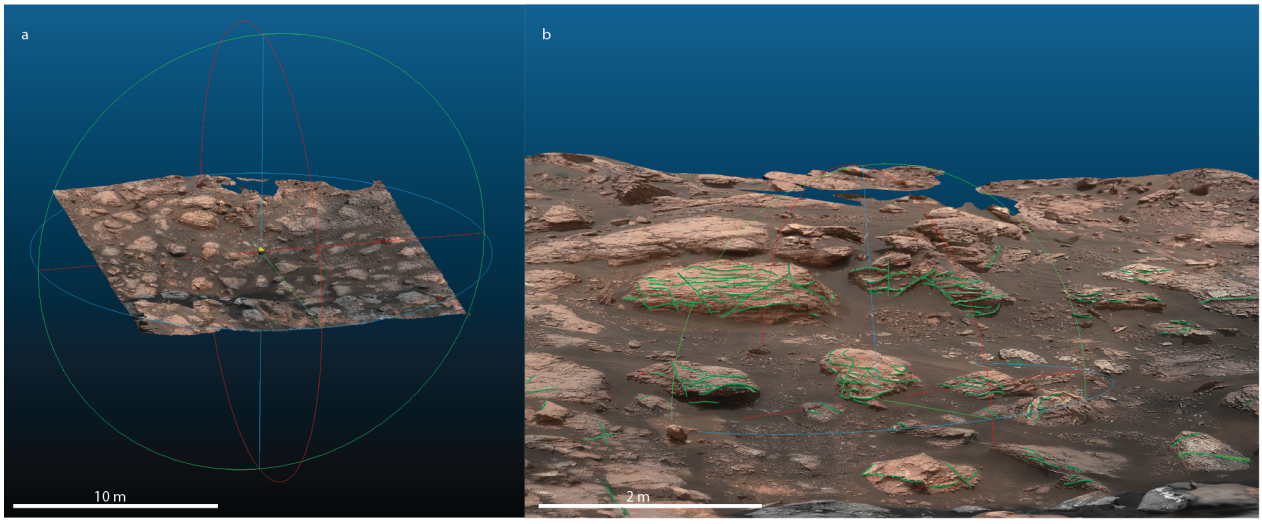

Figure 2. (a) 3D Digital Outcrop Model (DOM) of the region of interest within the area that Curiosity rover observed between sol 1536 and 1545. (b) Magnification of a portion of the study area; veins are highlighted in green above the texture.

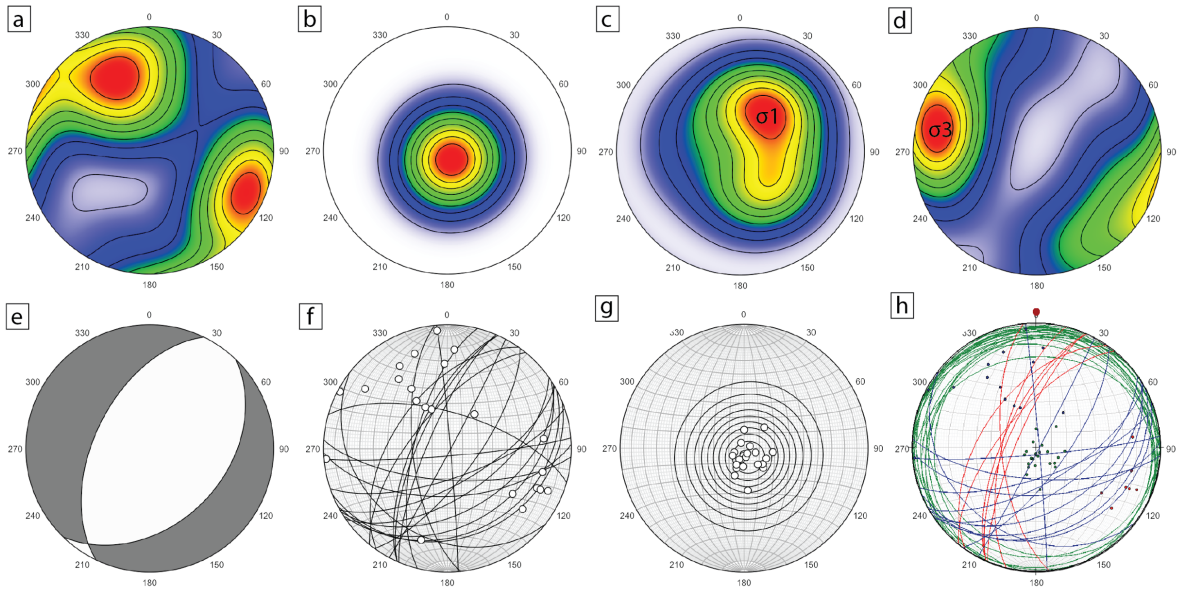

Figure 3. The stereo plots show: the orientation of the oblique (a,f), bedding-parallel (b,g) and entire population (h) fracture planes detected on the study area on Mars; the maximum and minimum stress orientations (c,d), the kinematics extracted from the oblique vein set's data (e). Dataset extracted from the 3D DOM: 46 planes.

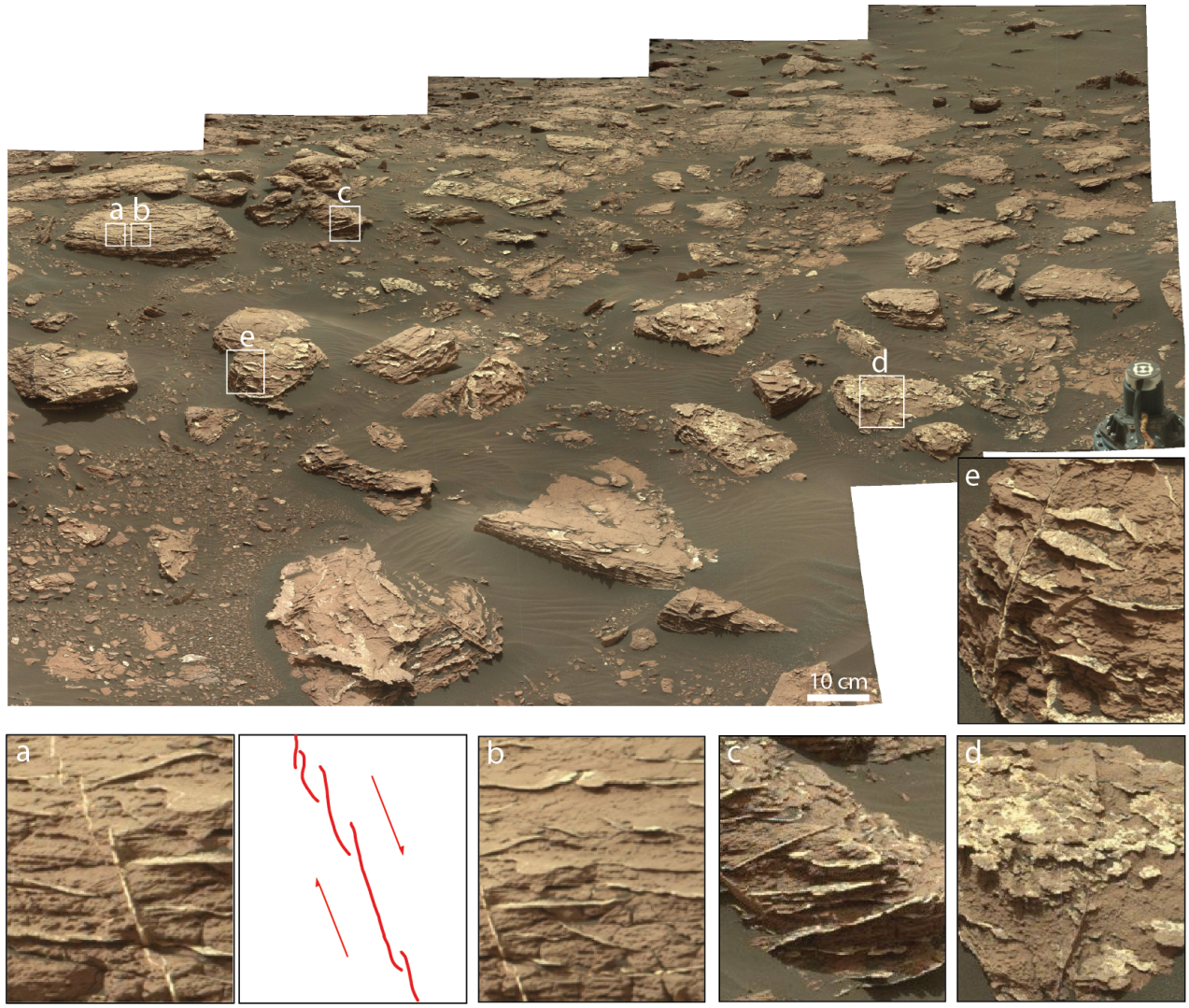

Figure 4. Stitched landscape of the main outcrops within the area of interest. Highlights on key traits: (a) recorded and preserved oblique set of veins showing “en-echelon” structures (magnification and sketch); (b, c) veins following the crosscutting lamination trend; (d, e) crosscutting relationship between horizontal and oblique sets.